

Near Threshold Computation of Partitioned Ring Learning With Error (RLWE) Post Quantum Cryptography on Reconfigurable Architecture

Paresh Baidya¹, Swagata Mondal², Rourab Paul³,

*Department of CSE, Siksha O Anusandhan (Deemed to be University), Bhubaneswar, Odisha India Siksha O Anusandhan, Bhubaneswar, India^{1,3},
Dept. Electronics and Communication, Jalpaiguri Government Engineering College, Maulana Abul Kalam Azad University²*

Abstract

Ring Learning With Error (RLWE) algorithm is used in Post Quantum Cryptography (PQC) and Homomorphic Encryption (HE) algorithm. The existing classical crypto algorithms may be broken in quantum computers. The adversaries can store all encrypted data. While the quantum computer will be available, these encrypted data can be exposed by the quantum computer. Therefore, the PQC algorithms are an essential solution in recent applications. On the other hand, the HE allows operations on encrypted data which is appropriate for getting services from third parties without revealing confidential plain-texts. The FPGA based PQC and HE hardware accelerators like RLWE is much cost-effective than processor based platform and Application Specific Integrated Circuit (ASIC). FPGA based hardware accelerators still consume more power compare to ASIC based design. Near Threshold Computation (NTC) may be a convenient solution for FPGA based RLWE implementation. In this paper, we have implemented RLWE hardware accelerator which has 14 subcomponents. This paper creates clusters based on the critical path of all 14 subcomponents. Each cluster is implemented in an FPGA partition which has the same biasing voltage V_{ccint} . The clusters that have higher critical paths use higher V_{ccint} to avoid timing failure. The clusters have lower critical paths use lower biasing voltage V_{ccint} . This voltage scaled, partitioned RLWE can save ~6% and ~11% power in Vivado and VTR platform respectively. The resource usage and throughput of the implemented RLWE hardware accelerator is comparatively better than existing literature.

Keywords: FPGA partition, Low Power, Post quantum, Ring-learning with error

1. Introduction

Lattice based cryptography is currently considered as one of the most secure solutions as compared to classical cryptography schemes. The discrete logarithm (Elliptic Curve Cryptography), RSA and ECDSA classical schemes are used to secure Internet communications. These asymmetric key crypto-systems are based on the hardness of prime factor and discrete logarithm. However, asymmetric key crypto-systems are no longer secure under quantum attacks. Even in brute force, Grover's quantum algorithm [1] reduces the searching space of symmetric key cryptography: Advanced Encryption Scheme (AES) from $O(2^n)$ to $O(2^{n/2})$, where n is the key size. That means AES-256 is as secure as AES-128. However, no such computationally strong quantum computer has been developed yet. IBM and Google have claimed to develop such computationally extensive quantum computers within a few years. Post-quantum crypto algorithms generally deal with non-quantum operations but it strongly resists both classical and quantum attacks. Mainly there are four post quantum cryptography schemes: Code based cryptography, Lattice based cryptography, Hash based cryptography and Multivariate quadratic cryptography. Among all these schemes lattice based cryptography(LBC) is computationally efficient. In 2005, O. Regev [2] first introduced a lattice based cryptography schemes name as Learning with error (LWE). Later LBC becomes more popular for its significant theoretical progress [2, 3]. The LBC becomes more suitable for real life applications when it was implemented in software and hardware platform by articles [4, 5, 6, 7, 8]. On the other hand, post-quantum cryptography finds its application in more advanced schemes such as fully homomorphic encryption, which allows the operations on the encrypted data without revealing any information to the third party.

For hardware implementation of RLWE as PQC and RLWE as HE, designer can choose either FPGA or ASIC platform. In practical, FPGA based PQC and HE hardware accelerators like RLWE is much cost-effective compared

to ASIC. However, FPGA based hardware accelerator is less energy efficient compared to ASIC [9] because of its programmable switch. An experimental study [10] shows power consumption of 8 bit full adder in Xilinx XC4003A is 100 times more compared to CMOS ASIC platform. The implementation of 8-bit adder in FPGA platform consumed the power 4.2mW/MHz at 5V and the same implementation in ASIC consumed 5.5uW/MHz at 3.3V [10]. The power consumption of FPGA based design is crucial specially for battery powered embedded system. Near Threshold Computation (NTC) may be an appropriate solution to reduce the power consumption of FPGA based RLWE implementation.

To the best of our knowledge, all the implementations [5, 11, 4, 12] on RLWE focuses on the speed and resource optimization of the encryption and decryption scheme. The primary goal of this paper is to reduce the power consumption of the RLWE hardware.

1.1. Related Work

O. Regev [2] introduced the first hardness proof of LWE cryptography in 2005. Later, various hardware and software implementation of LWE were proposed. There are many literature which implemented various subcomponents of RLWE algorithm. The polynomial multiplication, polynomial division and gaussian sampler used to generate error polynomials are the most challenging subcomponents of RLWE. Howe et. al [11] proposed first hardware architecture for a standard lattice based cryptography (LWE) on a Spartan-6 FPGA platform on 2016. The primary contribution of this paper is area optimization of Gaussian Sampler by balancing area and performance. Poppelman et al. [13] reported a hardware implementations of gaussian sampler of RLWE accelerator. They implemented Cumulative Distribution Table (CDT) based Gaussian sampler on reconfigurable hardware. Additionally, authors compared CDT based gaussian sampler and Bernoulli sampler. Roy et al. [7] implemented gaussian sampler using Knuth Yao algorithm for sampling from the discrete gaussian distribution. Poppelman et al. [14] implemented a polynomial multiplier which stores all twiddle factors in a dedicated memory required for NTT computation. Article [5] reduces the key size of the conventional LWE schemes and implements a compact and efficient LWE hardware. The article [5] compared LWE hardware and software implementations with Lindner and Peikert's design [15]. Article [5] introduced LWE-matrix and LWE-polynomial and compared these variants of LWE. Article [5] discarded the idea of LWE-matrix because of its large area consumption, they have only implemented RLWE-polynomial. Poppelman et al. [4] implements an efficient hardware of RLWE on Virtex 6 FPGA which can fit on a low-cost Spartan-6 FPGA. This hardware accelerator improved the work of [5]. Article [6] proposed a lightest RLWE encryption scheme by reducing the resource, compared with the high speed implementation of [4]. Roy et al.[12] implemented a compact ring-LWE coprocessor on Virtex 6 FPGA where they optimized NTT polynomial multiplication and reduced the computation cost of the twiddle factors by avoiding the pre-computation overhead. A variation of the Native Title Research Unit (NTRU) Encrypt system with a quantum security reduction is used in [16]. Its security is based on the standard model's LWE problem in polynomial rings. All the above mentioned RLWE implementations have mostly focussed on area versus speed issue. More speed causes more area and more area causes more power consumption. Without affecting the datapaths (area vs speed), the conventional low power solutions mostly deal with clock gating, power gating, dynamic voltage and frequency islands, retention power gating, save and restore power gating architectures. To the best our knowledge. this is the first RLWE hardware accelerator based on dynamic voltage island concept where different voltage islands run with near threshold voltages

1.2. Proposed RLWE

The literature of RLWE competes the growing high speed applications by increasing throughput of the architecture. The throughput is mostly achieved by more parallelism which causes more power consumption. Power consumption is a severe concern for embedded systems but existing literature has not explored the possibilities of Near Threshold Computation (NTC) in any PQC implementation. To the best of our knowledge our proposed RLWE is the first NTC in FPGA/ASIC platform. In our implementation we designed a RLWE dedicated hardware which has 14 subcomponents. The critical path of all these subcomponents are measured and based the value of critical path 4 cluster algorithms create groups with these 14 subcomponents. The FPGA is partitioned and different partitions has different biasing voltage V_{ccint} . The group having higher value of critical path is placed in a partition which have higher V_{ccint} and the group having lower value of critical path is placed in a partition which have lower V_{ccint} . The primary contribution of our paper is stated below:

- This paper designs and implements RLWE crypto algorithm in Artix-7 (28nm) FPGA. The RLWE has 14 subcomponents such as Random Number Generator (RND), Poly_div, NTT Controller, Polynomial Multiplier, Read only Memory (ROM), Scanner, Datapath Controller, Convolution Controller, Poly_add, reader, Distance, Row Column Controller and 2 dual port Random Access Memory (RAM).
- The cluster algorithms create groups of subcomponents which have similar critical paths. Each group are placed in a partitioned FPGA where each partition runs with different V_{ccint} . The group(s) with lower critical path(s) is placed in a lower V_{ccint} partition and the group(s) with higher critical path(s) is placed in a higher V_{ccint} partition.
- The proposed FPGA based voltage scaled RLWE can save 11% power consumption in VTR tool. The throughput, resource and power consumption of proposed RLWE is reasonably better compared to existing RLWE.

The rest of the paper is organised as follows: Sec. 2 states the background of the RLWE algorithm followed by Sec. 3 which gives a preliminary idea about hardware implementation of RLWE. Next, in Sec. 4, the The tool flow of the proposed model is described. In Sec. 5, the four cluster algorithm used to partition the FPGA is discussed and in Sec. 6.1 and Sec. 7, the proposed algorithm to calculate biasing voltage and results are stated respectively. Finally, Sec. 8. concludes the paper

2. The Ring-LWE Schemes

The Learning With Error (LWE) was proposed by O Regev in [2] 2005. The LWE become popular because it is developed in secure lattice based cryptosystem which resists quantum attacks. Later LWE achieves computational efficiency and it reduces the key size by adopting polynomial Ring [17]. The LWE schemes perform in $R_q = \mathbb{Z}_q[x]/\langle f \rangle$, where f is irreducible polynomial of degree $n - 1$, and $n = 2^k \geq 1$ and a prime q is chosen such a way that $q \equiv 1 \pmod{2n}$. There is an error distribution called discrete Gaussian distribution χ_σ with the standard deviation $\sigma > 1$ and mean 0. The LWE scheme defined as follows:

- KeyGEN(a): choose $r_1, r_2 \in R_q$ sampled from χ_σ . Let $p = r_1 - a * r_2$. The public key is (a, p) and private key is r_2 . The polynomial $a \in R_q$ chosen uniformly during the key generation.
- EnCrypt(a, p, m): choose error polynomials $e_1, e_2, e_3 \in R$ sampled from χ_σ . Then compute the cipher text as a polynomial

$$c_1 = a * e_1 + e_2 \quad (1)$$

$$c_2 = p * e_1 + e_3 + \tilde{m} \quad (2)$$

where $\tilde{m} = \text{encode}(m)$ and c_1 and c_2 are the encrypted message.

- DeCrypt(c_1, c_2, r_2): Decryption process requires to compute below equation.

$$m' = c_1 * r_2 + c_2 \quad (3)$$

Thereafter, to get the original message m , it needs to decode m' .

3. Hardware Architecture of RLWE

The proposed RLWE has 14 components such as Random Number Generator (RND), Polynomial Divider (Poly_Div), NTT Controller, Polynomial Multiplier, Polynomial Subtraction (Sub_mod), Scanner, Datapath Controller, Convolution Controller, Polynomial Adder (Poly_add), reader, Distance, Row Column Controller and 2 dual port Random Access Memory (RAM). The main components in the architecture are: the memory file, Gaussian sampler, random number generator, NTT controller and datapath controller. The brief description of all hardware components are stated below:

3.1. Random Number Generator (RND)

This paper uses Trivium Random [18] number generator to generate error polynomial e_3 . In our application the secret key required for the RLWE is predefined. In real application the secret key should be generated randomly which can be done by the Trivium Random Number Generator. Trivium require one key and initialize vector to generate random numbers.

3.2. Polynomial Divider (*poly_div*)

The polynomial divider is required to divide polynomials. The resultant value of all the arithmetic operations stated in equ. 1, equ. 2 and equ. 3 need to bring under $R_q = \mathbb{Z}_q[x] / \langle f \rangle$.

3.3. Dual Port RAM

This ram stores the public key, message, gaussian sample value required for RLW execution.

3.4. Datapath Controller

The Datapath Controller has three sub components such as: *Polynomial Multiplier*, *Polynomial Adder* (*poly_add*) and *Polynomial Subtraction* (*Sub_mod*) which are used to multiply, addition and subtraction of the polynomials.

3.4.1. Polynomial Multiplier

The polynomial multiplier (*poly_mul*) is required to multiply a and e_1 in equ. 1 and p and e_1 in in equ. 2

3.4.2. Polynomial Adder (*poly_add*)

The polynomial Adder (*Poly_add*) is required to add polynomials $a * e_1$ and e_2 in equ. 1 and $p * e_1$, e_3 and \tilde{m} in equ. 2.

3.4.3. Polynomial Subtraction (*Sub_mod*)

The Polynomial Subtraction (*Sub_mod*) is required to subtract polynomials. This block is required when Polynomial Divider (*poly_div*) will perform.

3.5. Convolution Controller

The convolution controller decides whether addition or multiplication will be executed. This block used to control the Datapath Controller.

3.6. reader

The reader block perform loading operation to load the coefficients of polynomials and Gaussian noise coefficients. It also encode the message bit before make into cipher text.

3.7. NTT Controller

In RLWE scheme, polynomial multiplication is one of the the main operation of the encryption and decryption process. hardware implementation of coefficient wise multiplication of two polynomial functions is computationally expensive. Therefore, we convert the coefficient wise representation to point wise representation using the Number Theoretic Transformation (NTT). *NTTController* performs the NTT operation on the polynomial functions a, p, r_2, e_1, e_2, e_3 to generate $\tilde{a}, \tilde{p}, \tilde{r}_2, \tilde{e}_1, \tilde{e}_2, \tilde{e}_3$.

3.8. Gaussian Sampler: *scanner, distance, row column controller*

The Gaussian Sampler is based on Knuth Yao Sampler [19]. The Knuth Yao Sampler is a tree based sampler which stores the binary expansion of the samples in a probability matrix. This probability matrix stores probabilities of the samples. Roy et al.[7] implemented the first hardware of Gaussian sampler using Knuth Yao algorithm which used pre-computed table of the probability matrix. Knuth Yao algorithm uses a random walk model for sampling process. This sampling process creates a discrete distribution generating (DDG) tree using the probability matrix. Our *Gaussian Sampler* has three subcomponents such as: *scanner, distance, row column controller* modules which are dedicated for traversing the tree, scanning the bit from the ROM and calculate the distance in the tree of visited node and intermediate node. The detail of the Knuth Yao sampler and DDG tree are describe in [19].

3.8.1. Scanner

Scanner block performs the scanning operation on the ROM block. It scans the bits from a ROM word. When all bits are read from a ROM word then it fetch next ROM word to scan.

3.8.2. Row ColumnController

Row ColumnController has two registers: an up counter named as *column_length* and a down counter named as *row_number*. The *column_length* stores the length of the different column length of the probability matrix. At the first step of column scanning process, *row_number* is initialized by the *column_length*. If the *row_number* reaches to zero, the column scanning process is completed.

3.8.3. Distance

The distance block requires to construct the DDG tree of the probability matrix. For this purpose a subtracter is used to control the random walk. When the subtracter value is < 0 , then it indicates completion of the sampling operation. After the completion of the sampling operation, the *row column controller* selects current *row_number* as a sample output.

4. Tool Flow

This paper uses two environments 1)Python-Vivado and 2) Python-VTR. In Python-Vivado environment, the vivado generates the synthesis report which includes timing report of RLWE. The timing report consists of all timing related information of RLWE including the critical path length of all design paths. This timing report is sent to python environment to cluster the 14 subcomponents of RLWE using cluster algorithms mentioned in Sec. 5. This python environment generates the Xilinx Design Constraints (XDC) file which mentions coordinates of all 14 subcomponent of RLWE in FPGA floor. This coordinates of RLWE subcomponents are generated based on the partition or cluster. This XDC then includes in the implementation process of *Vivado* environment. The *Vivado* used Artix 7, 28 nm FPGA. The VTR [20] also uses the same process as mentioned for *Vivado*. VTR generates Synopsys Design Constraint (SDC) file instead of XDC. The VTR uses 3 academic FPGAs : 22nm, 45nm and 180nm.

5. Cluster Algorithms

This paper analyses four clustering algorithms to group the different sub components of RLWE hardware accelerator. All these four algorithms follow different set of rules to find the similarity of the data in the data distribution. Based on our design requirements this paper implements four algorithms as stated below:

5.1. K-Means Clustering

K-Means clustering algorithm performs on data to find K division to satisfy a certain criterion. Firstly, it computes the distance between the data points and the randomly initialized centroids [21], then accordingly form the cluster of all the data which are close to the center. This iterative process is repeated until the criterion of the functions converges to the local minimum. Euclidean distance is used to compute distances between the data and its time complexity is $O(Kn)$, where K number of cluster and n number of data.

5.2. DBSCAN

The DBSCAN algorithm works on the assumption that clusters are in high-density regions and outliers tend to be in low-density regions. Unlike the K-Means algorithm, DBSCAN does not require the declaration of number of clusters beforehand. This algorithm finds the number of clusters [22] based on two parameters **epsilon** and **minpoint**. The **epsilon** : is a radius of the circle around a particular point that is to be considered as in the neighborhood of the other point. The **minpoint** : is the threshold on the least number of points in the circle to be considered as core points. To find the cluster DBSCAN choose any arbitrary point p that has not been visited before and takes all the points density-reachable from p with respect to epsilon and minpoints then a cluster is started. If there are less number of points than the minpoints, p point consider noise. In a newly created cluster, if all points are marked as accessed, then

same process used to deal with unvisited points and create a new cluster. This process will continue until all points are marked in cluster or noise. The main advantage of DBSCAN algorithm over the other algorithm is that it can identify the outlier point as a noise. The time complexity of this algorithm is $O(n)$ for reasonable epsilon.

5.3. Mean-Shift Clustering

Mean Shift Clustering [23] algorithm is based on the concept of Kernel Density Estimation (KDE). KDE assumes that the data points are sampled from a probability distribution and estimate the distribution by a weight function named as Kernel on each point in the data set. Among many kernels, the Gaussian kernel is the most popular. The mean shift algorithm works in such a way that the points climb uphill to the nearest peak on the KDE surface by iteratively shifting each point of the data set. It starts with a selected random point as the center of the kernel considering a circle having a certain radius in the data set. The kernel is then moved towards a higher density region by shifting the centroid to the mean of the points within the circle of the center. The mean shift clustering does not need prior knowledge of the number of clusters. It needs only one parameter: bandwidth to determine the number of clusters. This clustering algorithm is computationally expensive compared to K-means algorithm, time complexity in lower dimensions is $O(n * \log(n))$.

5.4. Hierarchical Clustering

The Hierarchical clustering [24] algorithm start with every point is its own cluster and compute distance matrix between two clusters based upon chosen distance measurement method(in this case Euclidean distance). Then it choose two clusters to be merged that has the smallest distance. This process will repeat until all clusters grouped into a single cluster. The dendrogram creates a binary tree for visualizing the hierarchy of clusters. The number of clusters can be determine from the dendrogram. This algorithm is computationally expensive for large datasets, having a time complexity of $O(n^3)$ where n is the number of data-points.

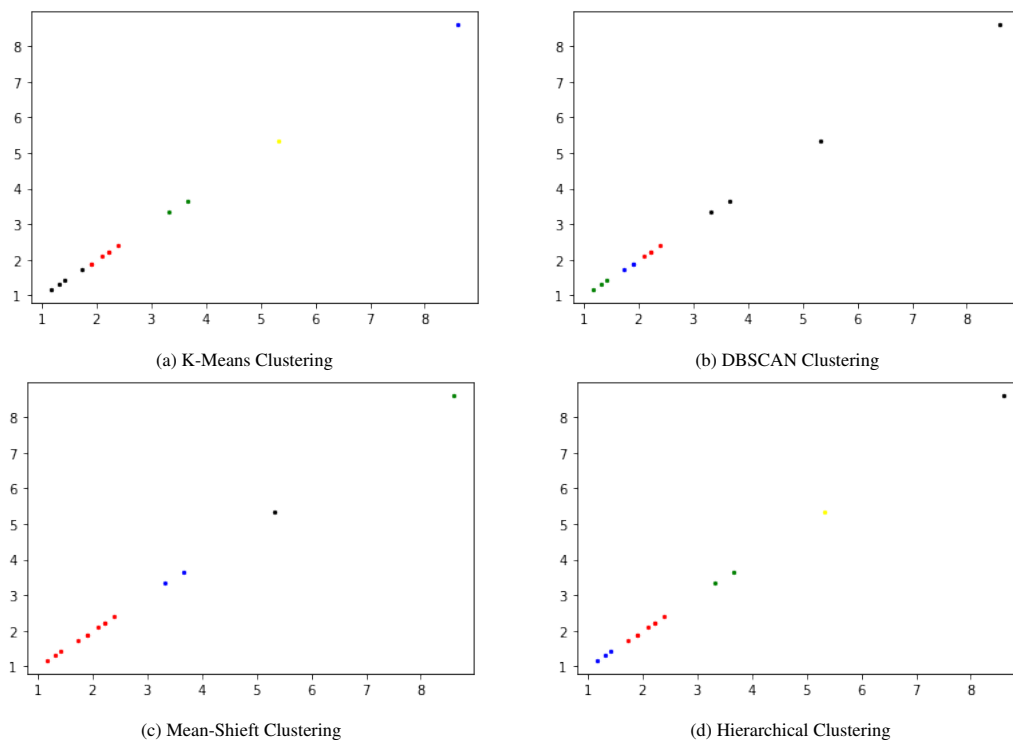


Figure 1: Clustering Algorithms

6. Voltage Calibration and ErrorControl Unit

The most challenging part of NTC is (i)Actual voltage allocation for specific FPGA partition and (ii)Run time timing errors.

6.1. Offline Voltage Calibration Algorithm

The proposed voltage scaled RLWE has 14 hardware components. These hardware components have different critical paths. The 4 cluster algorithms mentioned in Sec. 5 group these 14 components in different voltage island. Each FPGA partition has different biasing voltage V_{CCint} . The designer knows if the critical path of a hardware components is more, it needs more amount of V_{CCint} to avoid timing failure. However, designer does not know the actual amount of V_{CCint} required for particular length of critical path. This calibration of V_{CCint} depends on several design constraints, such as number of partition P , critical path C_i and critical region ($V_{ccintmax} - V_{ccintmin}$) as shown in Fig. 2. This Offline Voltage Calibration Algorithm has two parts: (i)Average Critical Path of each Partition shown in Algorithm 1 (ii)Voltage Scaling of each Partition shown in 2.

Calculation of average critical path CP_k describes in Algorithm. 1. Total critical path $A_{critical}$ of each partition is computed in Line 4 of Algorithm. 1. Thereafter, Line 6 calculates the average critical path CP_k of k^{th} partition based on $A_{critical}$ and number of components $N(k)$ in k^{th} partition. The distributed scaled voltage VP_k for each partition is computed by Algorithm. 2. It calculates voltage $V_{r/c}$ for per unit critical path from $V_{ccintmax}$ and $V_{ccintmin}$ as shown in Line 5. After that, the VP_k of the k^{th} partition is calculated depends on the $V_{r/c}$, average critical path CP_k and $V_{ccintmin}$.

6.2. Timing Errors

Despite of accurate V_{CCint} allocation, NTC on RLWE may causes timing errors. This paper designs a timing error control unit which uses razor flip in the datapath of each RLWE subcomponents. The razor or shadow flipflop in FPGA platform is driven by a delayed clock [25]. We have assumed that one or more timing pathways leading from any of the source registers terminate at a circuit register R . The shadow register S samples the same data as the main register R , but it does so on a delayed clock $DCLK$ that is delayed from CLK by T_{del} . Any data that enters the circuit after R samples but prior to S samples will result in a disparity between the two registers, which is identified by the error flag F . This razor flipflop is put in the datapaths of the subcomponents. Razor increases the resource consumption, but it also has the ability to detect runtime timing errors in RLWE caused by near-threshold biasing voltage. Fig.3 displays the timing diagram for the razor.

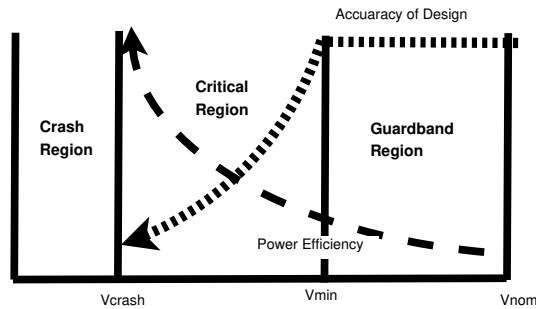


Figure 2: Voltage behaviour for V_{CCint}

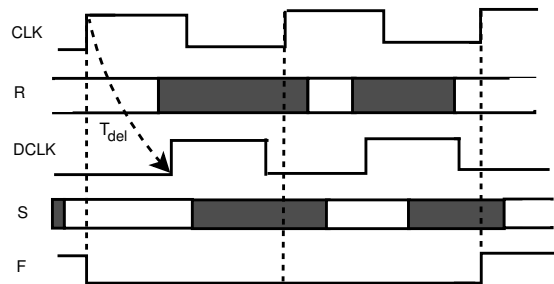


Figure 3: Razor Timing Diagram of Fault Detection

Table 1: K-Means Cluster

# Partition	Hardwares	Critical Paths(ns)	$V_{ccint}(Volt)$
1	Dual port ram:1	2.217	0.96
	Dual port ram:2	2.217	
	Row Column Controller	1.9	
	Distance	1.9	
	reader Wrapper	2.394	
	Poly_add	2.101	
2	Datapath	8.603	1.00
3	Scanner	3.332	0.97
	ROM	3.654	
4	Polynomial multiplier	5.327	0.98
5	NTT Controller	1.17	0.95
	Convolution Controller	1.725	
	Poly_div	1.323	
	rand	1.412	

Table 2: DBSCAN Cluster

# Partition	Hardwares	Critical Paths(ns)	$V_{ccint}(Volt)$
1	Dual port ram:1	2.217	0.96
	Dual port ram:2	2.217	
	reader Wrapper	2.394	
	Poly_add	2.101	
2	Row Column Controller	1.9	0.96
	Distance	1.9	
	Convolution Controller	1.725	
3	Datapath	8.603	0.98
4	Scanner	3.332	0.97
	ROM	3.654	
5	Polynomial multiplier	5.327	0.97
6	NTT Controller	1.17	0.96
	Poly_div	1.323	
	rand	1.412	

Table 3: Mean-Shift Cluster

# Partition	Hardwares	Critical Paths(ns)	$V_{ccint}(Volt)$
1	Dual port ram:1	2.217	0.96
	Dual port ram:2	2.217	
	Row Column Controller	1.9	
	Distance	1.9	
	reader Wrapper	2.394	
	Poly_add	2.101	
	NTT Controller	1.17	
	Convolution Controller	1.725	
	Poly_div	1.323	
	rand	1.412	
2	Datapath	8.603	1.00
3	Scanner	3.332	0.97
	ROM	3.654	
4	Polynomial multiplier	5.327	0.98

Table 4: Hierarchical

# Partition	Hardwares	Critical Paths(ns)	V_{ccint} (Volt)
1	Dual port ram:1	2.217	0.96
	Dual port ram:2	2.217	
	Row Column Controller	1.9	
	Distance	1.9	
	reader Wrapper	2.394	
	Poly_add	2.101	
	Convolution Controller	1.725	
2	Datapath	8.603	0.98
3	Scanner	3.332	0.97
	ROM	3.654	
4	Polynomial multiplier	5.327	0.98
5	NTT Controller	1.17	0.96
	Poly_div	1.323	
	rand	1.412	

Algorithm 1 Average Critical Path of each Partition

Require: n'_k, s, P $\triangleright k \leftarrow 0, 1, 2, \dots, P$

- 1: $A_{Critical} \leftarrow 0$
- 2: **for** $k \leftarrow 1$ to P **do**
- 3: **for** $i \leftarrow 1$ to $N(k)$ **do**
- 4: $A_{Critical} \leftarrow A_{Critical} + C_i$
- 5: **end for**
- 6: $CP_K \leftarrow A_{Critical}/N(k)$
- 7: **end for**

Algorithm 2 Voltage Scaling of each Partition

Require: $V_{ccint_{max}}, V_{ccint_{min}}, CP'_K, s$ $\triangleright k \leftarrow 0, 1, 2, \dots, P$

- 1: $T_{Critical} \leftarrow 0$
- 2: **for** $k \leftarrow 1$ to P **do**
- 3: $T_{Critical} \leftarrow T_{Critical} + CP_K$
- 4: **end for**
- 5: $V_{r/c} \leftarrow \frac{V_{ccint_{max}} - V_{ccint_{min}}}{T_{Critical}}$
- 6: **for** $k \leftarrow 1$ to P **do**
- 7: $VP_k \leftarrow V_{ccint_{min}} + CP_K * V_{r/c}$
- 8: **end for**

7. Result and Implementation

The aforementioned 5 cluster algorithms are implemented by Python using the Scikit-learn library for two environments (i) Commercial Vivado tool with Artix-7 FPGA (ii) VTR tool for 22nm, 45nm and 130nm academic FPGAs. This paper proposes two different architectures of RLWE encryption [12] scheme for the parameter set $(n, q, s) : (256, 7681, 11.32)$. The first approach implements RLWE hardware accelerator without voltage scaling, whereas the second RLWE architecture is designed with different voltage partitions. Presently, there is no FPGA which supports multiple V_{ccint} . Therefore, the power results are carried out separately where one partition is considered as individual circuit. These two designs are studied in two voltages regions. The V_{ccint} of each partitions are calculated by algorithm 1 and 2.

7.1. Vivado and VTR: Voltage Region: $V_{ccint_{min}} = 0.95$ volt to $V_{ccint_{max}} = 1.05$ volt

The guard band voltage region of Artix-7 is $V_{ccint_{min}} = 0.95$ volt to $V_{ccint_{max}} = 1.05$ volt. Though academic FPGAs on VTR platform supports voltages of critical region, for sake of better comparative study we have implemented 14 components of RLWE with voltage range of $V_{ccint_{min}} = 0.95$ volt to $V_{ccint_{max}} = 1.05$ volt for both *Vivado* and *VTR*. Table 5 shows *Vivado* 28nm Artix-7, *VTR* 22nm, *VTR* 45nm and *VTR* 130nm can save 4.34%, 1.19%, 1.18% and 1% power respectively.

7.2. VTR: Voltage Region: $V_{ccint_{min}} = 0.5$ volt to $V_{ccint_{max}} = 1.3$ volt

Unlike *VTR*, *Vivado* does not allow any V_{ccint} below 0.95 and above 1.05. As shown in Table 6, different number of clusters generated from K-Means, Mean-Shift, DBScan and Hierarchical algorithms consider voltage region from $V_{ccint_{min}} = 0.5$ volt to $V_{ccint_{max}} = 1.3$ volt for 22nm, 45nm and 130nm in VTR flow.

Table 5: Power Consumption of Vivado and VTR : Voltage Region: $V_{ccint_{min}} = 0.95$ volt to $V_{ccint_{max}} = 1.05$

Our Design Under 25° Ambient Temperature & 100 MHZ Clock	Cluster algorithms	Partition No.	V_{ccint_i} Volt	Vivado 28nm	VTR 22nm	VTR 45nm	VTR 130nm
Without Voltage scaling	NA	NA	1.00	22.45	46.44	59.09	190.38
Voltage scaled	K-Means	Partition-1	0.96	21.48	45.89	58.402	188.49
		Partition-2	1.00				
		Partition-3	0.97				
		Partition-4	0.98				
		Partition-5	0.95				
% of Reduction				4.34	1.19	1.18	1.005
Without Voltage scaling	NA	NA	1.00	22.45	46.44	59.09	190.38
Voltage scaled	Mean-Shift	Partition-1	0.96	21.62	45.94	58.46	187.2
		Partition-2	0.97				
		Partition-3	1				
		Partition-4	0.98				
% of Reduction				3.73	1.1	1.09	1.69
Without Voltage scaling	NA	NA	1.00	22.45	46.44	59.09	190.38
Voltage scaled	DBSCAN	Partition-1	0.96	21.16	45.87	58.38	188.5
		Partition-2	0.96				
		Partition-3	0.97				
		Partition-4	0.98				
% of Reduction				5.78	1.24	1.21	0.99
Without Voltage scaling	NA	NA	1.00	22.45	46.44	59.09	190.38
Voltage scaled	Hierarchical	Partition-1	0.96	21.62	45.94	58.46	188.6
		Partition-2	0.96				
		Partition-3	0.97				
		Partition-4	0.98				
		Partition-5	1				
% of Reduction				3.73	1.1	1.09	0.93

As an example, K-Means algorithm generates five partitions. Algorithm 1 calculates average critical path CP_k of the k^{th} partition where $A_{Critical}$ is the total critical path the k^{th} partition. Then algorithm 2 first computes the voltage per unit critical path $V_{r/c}$, after that required biasing voltage VP_k for k^{th} partition is calculated in line 7 of algorithm 2. The five V_{ccint} s calculated by algorithm 2 using K-Means are : $V_{ccint_1} = 0.96$ $V_{ccint_2} = 0.995 \approx 1$, $V_{ccint_3} = 0.965 \approx 0.97$ $V_{ccint_4} = 0.975 \approx 0.98$, $V_{ccint_5} = 0.955 \approx 0.95$. In Table 5, our voltage scaling method in same voltage ranges, reduces the dynamic power consumption 3.73% to 5.78% in Vivado environment and reduces 0.93% to 1.24% in VTR environment. Table 6 shows adoption of voltage scaling technology reduces dynamic power consumption 10.19% to 11.15%, 9.83% to 10.82% and 4.82% to 6.38% for 22nm, 45nm and 130nm VTR flow respectively.

Table 6: Power Consumption for VTR, Voltage Region: $V_{ccint_{min}} = 0.5$ volt to $V_{ccint_{max}} = 1.3$

Our Design Under 25° Ambient Temperature & 100 MHZ Clock	Cluster algorithms	Partition No.	V_{ccint_i} Volt	VTR 22nm	VTR 45nm	VTR 130nm
Without Voltage scaling	NA	NA	1.00	46.44	59.09	190.38
Voltage scaled	K-Means	Partition-1	0.96	41.41	52.69	179.55
		Partition-2	1.00			
		Partition-3	0.97			
		Partition-4	0.98			
		Partition-5	0.95			
% of Reduction				10.83	10.82	5.68
Without Voltage scaling	NA	NA	1.00	46.44	59.09	190.38
Voltage scaled	Mean-Shift	Partition-1	0.96	41.71	53.28	181.2
		Partition-2	0.97			
		Partition-3	1			
		Partition-4	0.98			
% of Reduction				10.19	9.83	4.82
Without Voltage scaling	NA	NA	1.00	46.44	59.09	190.38
Voltage scaled	DBSCAN	Partition-1	0.96	41.27	52.77	178.2
		Partition-2	0.96			
		Partition-3	0.97			
		Partition-4	0.98			
% of Reduction				11.15	10.71	6.38
Without Voltage scaling	NA	NA	1.00	46.44	59.09	190.38
Voltage scaled	Hierarchical	Partition-1	0.96	41.48	53	181.1
		Partition-2	0.96			
		Partition-3	0.97			
		Partition-4	0.98			
		Partition-5	1			
% of Reduction				10.69	10.32	4.89

Table 7: Compare between Vivado and VTR

Designs	Slice Register	Slice LUT	DSP	BRAM	Critical Path (NS)	Throughput
Our Design	665	846	2	1	2.539	
[4]	1506	4549	1	12		
[26]-V1	1624	4365	1	5		
[26]-V2	2122	5616	6	8		
[27]	-	1349	1	2		
[28]512	1145	3228	4	7		
[28]256	640	1637	4	5.5		

8. Conclusion

This paper implements a low power RLWE hardware accelerator in Artix-7 28nm commercial FPGA, 22nm, 45nm and 130 nm academic FPGA using *Vivado* and *VTR* tool. The proposed methodology creates clusters of the subcomponents of RLWE based on its critical path. The FPGA floor is partitioned and each cluster is placed in each FPGA partition. The clusters which have higher average critical path is connected with higher biasing voltage and the clusters which have lower average critical path is connected with lower biasing voltage to avoid the timing failure. This paper proposes an algorithm to calculate the actual biasing voltage required for certain amount of average critical path of a partition based in the available FPGA technology ($V_{ccint,max}$, $V_{ccint,min}$) and number of partitions. This voltage scaled, partitioned RLWE can save $\sim 6\%$ and $\sim 11\%$ power in Vivado and VTR platform respectively. The resource usage and throughput of the implemented RLWE hardware accelerator is comparatively better than existing literature.

References

- [1] Markus Grassl, Brandon Langenberg, Martin Roetteler, and Rainer Steinwandt. Applying grover’s algorithm to aes: quantum resource estimates. In *Post-Quantum Cryptography*, pages 29–43. Springer, 2016.
- [2] Oded Regev. On lattices, learning with errors, random linear codes, and cryptography. In *Proceedings of the thirty-seventh annual ACM symposium on Theory of computing*, pages 84–93, 2005.
- [3] Daniele Micciancio and Oded Regev. Lattice-based cryptography. In *Post-quantum cryptography*, pages 147–191. Springer, 2009.
- [4] Thomas Pöppelmann and Tim Güneysu. Towards practical lattice-based public-key encryption on reconfigurable hardware. In *International Conference on Selected Areas in Cryptography*, pages 68–85. Springer, 2013.
- [5] Norman Göttert, Thomas Feller, Michael Schneider, Johannes Buchmann, and Sorin Huss. On the design of hardware building blocks for modern lattice-based encryption schemes. In *International Workshop on Cryptographic Hardware and Embedded Systems*, pages 512–529. Springer, 2012.
- [6] Thomas Pöppelmann and Tim Güneysu. Area optimization of lightweight lattice-based encryption on reconfigurable hardware. In *2014 IEEE international symposium on circuits and systems (ISCAS)*, pages 2796–2799. IEEE, 2014.
- [7] Sujoy Sinha Roy, Frederik Vercauteren, and Ingrid Verbauwhede. High precision discrete gaussian sampling on fpgas. In *International Conference on Selected Areas in Cryptography*, pages 383–401. Springer, 2013.
- [8] Aydin Aysu, Cameron Patterson, and Patrick Schaumont. Low-cost and area-efficient fpga implementations of lattice-based cryptography. In *2013 IEEE international symposium on hardware-oriented security and trust (HOST)*, pages 81–86. IEEE, 2013.
- [9] Paul S Zuchowski, Christopher B Reynolds, Richard J Grupp, Shelly G Davis, Brendan Cremen, and Bill Troxel. A hybrid asic and fpga architecture. In *IEEE/ACM International Conference on Computer Aided Design, 2002. ICCAD 2002.*, pages 187–194. IEEE, 2002.
- [10] E. Kusse and J. Rabaey. Low-energy embedded fpga structures. In *Proceedings. 1998 International Symposium on Low Power Electronics and Design (IEEE Cat. No.98TH8379)*, pages 155–160, 1998.
- [11] J. Howe, C. Moore, M. O’Neill, F. Regazzoni, T. Güneysu, and K. Beeden. Lattice-based encryption over standard lattices in hardware. In *2016 53rd ACM/EDAC/IEEE Design Automation Conference (DAC)*, pages 1–6, 2016.
- [12] Sujoy Sinha Roy, Frederik Vercauteren, Nele Mentens, Donald Donglong Chen, and Ingrid Verbauwhede. Compact ring-lwe cryptoprocessor. In *International workshop on cryptographic hardware and embedded systems*, pages 371–391. Springer, 2014.
- [13] Thomas Pöppelmann, Léo Ducas, and Tim Güneysu. Enhanced lattice-based signatures on reconfigurable hardware. In *International Workshop on Cryptographic Hardware and Embedded Systems*, pages 353–370. Springer, 2014.
- [14] Thomas Pöppelmann and Tim Güneysu. Towards efficient arithmetic for lattice-based cryptography on reconfigurable hardware. In *International conference on cryptology and information security in Latin America*, pages 139–158. Springer, 2012.
- [15] Richard Lindner and Chris Peikert. Better key sizes (and attacks) for lwe-based encryption. In *Cryptographers’ Track at the RSA Conference*, pages 319–339. Springer, 2011.
- [16] Damien Stehlé and Ron Steinfeld. Making ntru as secure as worst-case problems over ideal lattices. In *Annual international conference on the theory and applications of cryptographic techniques*, pages 27–47. Springer, 2011.

- [17] Vadim Lyubashevsky, Chris Peikert, and Oded Regev. On ideal lattices and learning with errors over rings. In *Annual international conference on the theory and applications of cryptographic techniques*, pages 1–23. Springer, 2010.
- [18] Turgay Kaya. Memristor and Trivium-based true random number generator. *Physica A Statistical Mechanics and its Applications*, 542:124071, March 2020.
- [19] Donald E Knuth and YAO AC. The complexity of nonuniform random number generation. 1976.
- [20] Kevin E. Murray, Oleg Petelin, Sheng Zhong, Jia Min Wang, Mohamed Eldafrawy, Jean-Philippe Legault, Eugene Sha, Aaron G. Graham, Jean Wu, Matthew J. P. Walker, Hanqing Zeng, Panagiotis Patros, Jason Luu, Kenneth B. Kent, and Vaughn Betz. Vtr 8: High-performance cad and customizable fpga architecture modelling. *ACM Trans. Reconfigurable Technol. Syst.*, 13(2), May 2020.
- [21] David Arthur and Sergei Vassilvitskii. k-means++: The advantages of careful seeding. Technical report, Stanford, 2006.
- [22] Martin Ester, Hans-Peter Kriegel, Jörg Sander, Xiaowei Xu, et al. A density-based algorithm for discovering clusters in large spatial databases with noise. In *kdd*, volume 96, pages 226–231, 1996.
- [23] Dorin Comaniciu and Peter Meer. Mean shift: A robust approach toward feature space analysis. *IEEE Transactions on pattern analysis and machine intelligence*, 24(5):603–619, 2002.
- [24] D Manning Christopher, Raghavan Prabhakar, and Schütze Hinrich. Introduction to information retrieval, 2008.
- [25] D. Ernst, Nam Sung Kim, S. Das, S. Pant, R. Rao, Toan Pham, C. Ziesler, D. Blaauw, T. Austin, K. Flautner, and T. Mudge. Razor: a low-power pipeline based on circuit-level timing speculation. In *Proceedings. 36th Annual IEEE/ACM International Symposium on Microarchitecture, 2003. MICRO-36.*, pages 7–18, 2003.
- [26] Timo Zijlstra, Karim Bigou, and Arnaud Tisserand. Fpga implementation and comparison of protections against scas for rlwe. In *International Conference on Cryptology in India*, pages 535–555. Springer, 2019.
- [27] Ruan De Clercq, Oscar Reparaz, Sujoy Sinha Roy, Frédérik Vercauteren, and Ingrid Verbauwhede. Masking ring-lwe. *Journal of Cryptographic Engineering*, 6(2):139–153, 2016.
- [28] Markus Rückert and Michael Schneider. Estimating the security of lattice-based cryptosystems. *Cryptology ePrint Archive*, 2010.